Pitch Angle of Spiral Galaxies as Viewed from Global Instabilities of Flat Stellar Disks

Shunsuke Hozumi

Max-Planck-Institut für Astronomie, Königstuhl 17, D-69117 Heidelberg, Germany

Abstract. We investigate whether the behavior of the pitch angle, predicted by a local dispersion relation derived from the density wave theory, can be applied to that of the fastest growing, globally unstable modes of flat stellar disks. We pay attention to two-armed modes, and obtain such global modes by numerically integrating the linearized collisionless Boltzmann equation. The results show that the pitch angle of the fastest growing modes has a tight correlation with the ratio of the square of the radial velocity dispersion to the surface density, as indicated by the local theory, over a sufficiently wide range of radii. The correspondence between the global modes and global properties of spiral galaxies is briefly discussed.

1 Introduction

Spiral structure is one of the most prominent features in disk galaxies. In fact, Hubble [6] classified spiral galaxies on the basis of the observed appearance of spiral arms. However, what his classification scheme, known as the Hubble sequence, represents physically remains still unclear.

One of the most successful theories to understand spiral structure is the density wave theory, which was originally conceived by Lindblad [10], and was first formulated by Lin and Shu [9]. This theory was based on local analysis, so that owning to the inhomogeneous density distributions in galaxy disks, density waves are propagated with a group velocity, and disappear in a few dynamical times [20]. In addition, it is found that spiral shocks [15] induced by a gaseous component in the disk damp the underlying spiral potential, again on a dynamical time scale [8].

The difficulties confronted with the density wave theory mentioned above may be overcome by the concept of global modes. Indeed, global analysis of thin disks has revealed that many unstable modes exist in self-gravitating disks treated with a fluid approximation [1] and in those composed of stars [7]. In particular, Bertin et al. [2] have shown that all Hubble morphological types can be realized by global modes using fluid disk models with appropriate basic states. In their modal calculations, it is demonstrated that the pitch angle of global modes depends on a fraction of the active disk mass, the distribution of Toomre's Q parameter [19], the typical Q value, and so on. Since their major concern was to specify the basic state to generate and support a given spiral structure, they did not describe explicitly what determined the pitch angle of spiral arms.

Since the density wave theory gives, in general, a good description of real spiral galaxies [17], it can help us understand the physics of spiral structure in spite of a local theory based on a WKBJ approximation. However, it is not necessarily clear whether the properties of global modes can be fully described by local density waves (see [21]). In this paper, we first show what is predicted for the pitch angle of unstable modes on the basis of the density wave theory. Next, this prediction is examined for the fastest growing two-armed modes of stellar disks in a global context.

2 Prediction by the Density Wave Theory

For tightly wrapped spiral waves in a cool disk, the dispersion relation for a one-component fluid model [3] is given by

$$(\omega - m\Omega)^2 = c^2k^2 - 2\pi G\Sigma|k| + \kappa^2, \tag{1}$$

where ω, Ω, κ, k, c, G, Σ, and m are the wave frequency, angular speed of a star, epicyclic frequency, wavenumber, sound speed, gravitational constant, surface density of the disk, and number of arms in spiral patterns, respectively. Equation (1) is rewritten as

$$(\omega - m\Omega)^2 = c^2(|k| - \pi G\Sigma/c^2)^2 + \kappa^2\left(1 - 1/Q_{\rm g}^2\right), \tag{2}$$

where $Q_{\rm g} = \kappa c/(\pi G\Sigma)$ is the Toomre stability parameter for gas disks. When $Q_{\rm g} > 1$, all waves are stable, so that there is no specific wave to be selected. However, taking into account unstable waves, the wave mode with the highest growth rate should appear in the disk by overwhelming the others with time. Since the Toomre parameter is a criterion valid only for local axisymmetric Jeans instabilities, we neglect the stability condition that $Q_{\rm g} > 1$ in the case of non-axisymmetric instabilities like those two-armed modes focused on here, and will find what is expected if (2) includes unstable waves.

Equation (2) indicates that the most unstable wave has the wavenumber $|k_{\rm m}| = \pi G\Sigma/c^2$, which is converted to the wavelength $\lambda_{\rm m}$ given by

$$\lambda_{\rm m} = 2c^2/G\Sigma. \tag{3}$$

Thus, we can see that the wavelength of the most unstable mode depends on c^2/Σ. As the wavelength is larger, the pitch angle of spiral arms becomes larger. Therefore, the density wave theory predicts, as is well-known, that the pitch angle increases with increasing c^2/Σ.

3 Models and Method

Since we aim not at the reproduction of real spiral structures but at demonstrating how well and to what extent the local theory gives a representation of the features of global modes, we use disk models appropriate for our concern, irrespective of the deviation from realism.

We adopt infinitesimally thin Toomre disks [18] without bulges, whose surface density distributions, Σ, and potentials, Ψ, are given, respectively, by

$$\Sigma(R) = \frac{Mq}{2\pi a^2}\left(1+\frac{R^2}{a^2}\right)^{-3/2}, \tag{4}$$

and

$$\Psi(R) = -\frac{GM}{\sqrt{R^2+a^2}}, \tag{5}$$

where R is the distance from the center of the disk, and a is the length scale. Here, q $(0 < q \leq 1)$ represents an active disk mass fraction of the total mass. Since the Toomre disks are the flat version of Plummer's models [14] in three-dimensional configurations, for each disk model the fraction, $1-q$, of the total mass is considered to reside in a surrounding dark halo represented by a Plummer model with the same length scale a as that of the disk. Thus, in our models, the total mass distribution including a disk and a halo is identical, and the mass fraction of the disk is different.

For this mass profile, we can use Miyamoto's distribution functions (DFs) [12] with respect to directly rotating stars, $F^+(\varepsilon, j)$, where ε and j are the energy and angular momentum of a star per unit mass, respectively. Retrograde stars are introduced in the same manner as that adopted by Nishida et al. [13]. Then, the equilibrium DFs, F_0, are given by

$$F_0(\varepsilon, j) = \begin{cases} q[(1/2)F_0^+(\varepsilon) + F_1^+(\varepsilon, j)], & (j \geq 0) \\ (1/2)qF_0^+(\varepsilon), & (j < 0), \end{cases} \tag{6}$$

where the functions, $F_0^+(\varepsilon)$ and $F_1^+(\varepsilon, j)$, are derived from the expansion of $F^+(\varepsilon, j)$ as

$$F^+(\varepsilon, j) = F_0^+(\varepsilon) + F_1^+(\varepsilon, j). \tag{7}$$

The Miyamoto DFs [12] are characterized by the parameter n that specifies the distribution of radial velocity dispersion, c_r, such that

$$c_\mathrm{r}^2(R) = -\frac{1}{2n+4}\Psi(R). \tag{8}$$

This equation indicates that c_r can be provided independently of the disk surface density.

If disk models satisfy the condition such that $(n+2)q =$ constant, they have the same c_r^2/Σ distribution throughout the disk, as derived from (4), (5), and (8). We take $(n+2)q = 5$ with the pairs of $(n, q) = (3, 1)$, $(4, 5/6)$, $(5, 5/7)$, $(6, 5/8)$, $(7, 5/9)$, and $(10, 5/12)$, and $(n+2)q = 3$ with the pairs of $(n, q) = (3, 3/5)$, $(4, 1/2)$, $(5, 3/7)$, and $(6, 3/8)$. In Fig. 1, the distributions of the Q parameter for both model sequences are presented. Here, Q is defined for stellar disks as

$$Q = \frac{\kappa c_\mathrm{r}^2}{3.36 G\Sigma}. \tag{9}$$

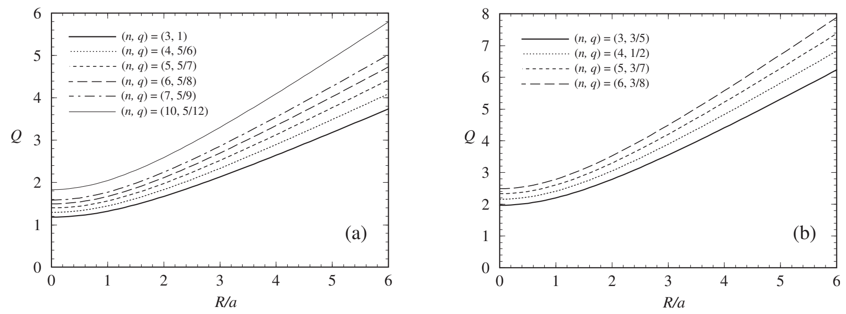

Fig. 1. Distribution of the Toomre stability parameter Q for (a) the models with $(n+2)q = 5$, and for (b) the models with $(n+2)q = 3$

It is found from this figure that all models are locally stable, i.e., $Q > 1$.

The most unstable global modes are obtained by numerically integrating the linearized collisionless Boltzmann equation given by

$$\frac{df_m}{dt} = \frac{\partial \psi_m}{\partial R}\frac{\partial F_0}{\partial u} + im\psi_m \frac{\partial F_0}{\partial j}, \tag{10}$$

where f_m and ψ_m are the perturbed distribution function and perturbed potential, respectively, with respect to the m-armed mode, and i is the unit of the imaginary part. Equation (10) is solved as an initial value problem by evolving an arbitrary form of perturbation, imposed initially, forward in time until it has reached the exponential growth in f_m and ψ_m. We restrict ourselves only to $m = 2$ modes, which are usually the most unstable modes among various m-armed modes. In fact, most of grand-design spirals show two-armed features. The numerical details are described in [5].

The units of mass and length, and the gravitational constant are taken so that $M = a = 1$ and $G = 1$, respectively. Then, the unit of time is $(a^3/GM)^{1/2}$.

4 Results

We have obtained the fastest growing two-armed modes of the models with $(n+2)q = 5$ and those with $(n+2)q = 3$. The growth rate, pattern speed, and corotation radius of each model are summarized in Table 1 for $(n+2)q = 5$, and in Table 2 for $(n+2)q = 3$.

We calculate the pitch angle, $i_{\rm p}$, given by

$$\cot i_{\rm p} = \left| mR\frac{\partial \phi}{\partial R} \right|, \tag{11}$$

where for a specified arm in the disk, ϕ is the phase angle of the density crest of the mode along R [3]. Here, we employ $m = 2$.

Table 1. Results for the fastest growing modes of the models with $(n+2)q = 5$

n	q	Growth Rate	Pattern Speed	Corotation Radius
3	1	0.224	0.333	1.83
4	5/6	0.167	0.328	1.85
5	5/7	0.119	0.313	1.92
6	5/8	0.0851	0.294	2.03
7	5/9	0.0652	0.275	2.15
10	5/12	0.0516	0.228	2.49

Table 2. Results for the fastest growing modes of the models with $(n+2)q = 3$

n	q	Growth Rate	Pattern Speed	Corotation Radius
3	3/5	0.0309	0.226	2.51
4	1/2	0.0158	0.213	2.62
5	3/7	0.00744	0.201	2.74
6	3/8	0.00449	0.190	2.86

The pitch angle of each mode, measured in degrees, is shown in Fig. 2, which illustrates that the pitch angle profile does not change substantially from model to model for each model sequence. For the $(n+2)q = 5$ sequence, all but the model with $(n,q) = (10, 5/12)$ have nearly the same pitch angle profile within $R = 5$. Even if the model with $(n,q) = (10, 5/12)$ is included in this sequence, the difference in pitch angle is rather small from $R \sim 2$ to $R \sim 5$. For the $(n+2)q = 3$ sequence, the pitch angles are not well determined because the very small growth rates do not enhance the density contrast of the unstable modes conspicuously. In spite of the large scatters, the pitch angles of these models appear to fluctuate around a certain profile. Therefore, also in this sequence, it can be found that the pitch angle profiles are approximately similar to one another. These results are remarkable in that models with different radial velocity dispersion profiles and different degrees of self-gravity show almost the same pitch angle profile over a sufficiently wide range of radii.

According to the local theory prediction, the increase in c_{r}^2/Σ leads to the increase in pitch angle, as found from (3) and (11). In our models, c_{r}^2/Σ is inversely proportional to $(n+2)q$, and so, the pitch angles for the $(n+2)q = 3$ sequence should be systematically larger than those for the $(n+2)q = 5$ sequence, as indicated by Fig. 3 (a), in which the pitch angles are calculated from (3) and (11). We can see this expected behavior in Fig. 3 (b), where the pitch angle profiles of all the models are put together. However, the difference in pitch angle

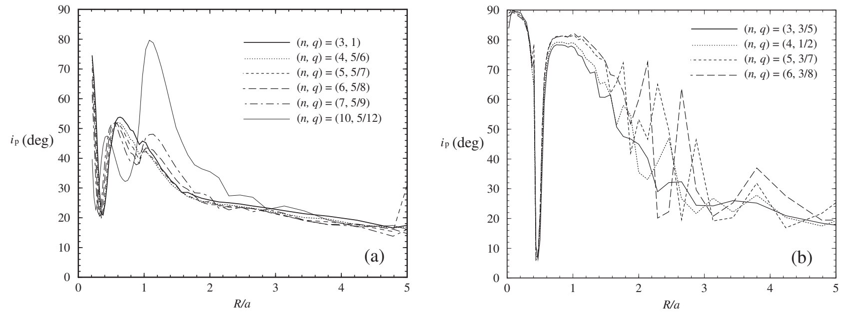

Fig. 2. Pitch angle of the fastest growing two-armed modes for (a) the models with $(n+2)q = 5$, and for (b) the models with $(n+2)q = 3$

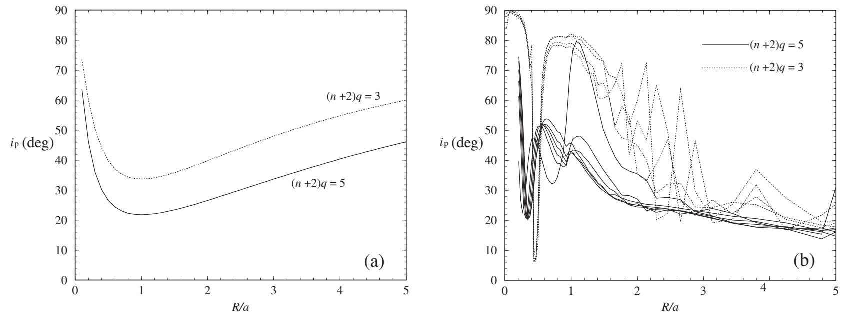

Fig. 3. Pitch angle of unstable two-armed modes for (a) expected profiles calculated from the local dispersion relation for $(n+2)q = 5$ (solid line), and for $(n+2)q = 3$ (dotted line), and for (b) obtained profiles of all the models with $(n+2)q = 5$ (solid lines) and $(n+2)q = 3$ (dotted lines)

for both model sequences becomes very small at larger radii than $R = 3$ unlike those values obtained from the local dispersion relation which are presented in Fig. 3 (a).

5 Discussion and Conclusions

We have found that the pitch angles of the fastest growing modes obey the prediction derived from the density wave theory even in a global context. We conclude from our global mode calculations that the pitch angles of spiral arms are regulated to a considerable degree by a typical value of c_{r}^2/Σ, if spiral structure is viewed as a manifestation of the fastest growing modes of stellar disks. In addition, our results indicate that the density wave theory is helpful to understand the properties of global modes qualitatively. In particular, although the theory is developed for tightly wound spirals, it is still useful for loosely wound spirals because the pitch angles obtained here are typically 20°.

Roberts and Haynes [16] have summarized the global properties of spiral galaxies along the Hubble sequence. According to their Fig. 2, there is no practically systematic change in total mass at least from Sa to Sc. Furthermore, their Fig. 3 illustrates that the total surface density including gaseous and stellar components decreases slightly from Sa to Sc. If the mass distributions of spiral galaxies would not change substantially, the decrease in total surface density and the increase in pitch angle, together with our results, suggest that c_{r} would be nearly constant or increase from Sa to Sc. Therefore, observations of c_{r} along the Hubble sequence will clarify the relevance of our argument.

Recently, Ma [11] has revealed that the pitch angle increases as the disk surface density decreases by analyzing all Hubble type galaxies altogether. Ma's finding is consistent with our results of global mode calculations. His analysis shows a large scatter in the relation between the pitch angle and the surface density. If a typical c_{r}^2/Σ instead of Σ was chosen for each spiral galaxy, this scatter might be reduced.

From the arguments mentioned above, real spiral structures appear to reflect the characteristics of the fastest growing, global modes of stellar disks. In fact, the old stellar population observed at near-infrared wavelengths forms large-scale smooth symmetric arms in the disk (e.g., [4]). These features may be a manifestation of globally unstable modes.

References

1. S. Aoki, M. Noguchi, M. Iye: Publ. Astron. Soc. Jpn. **31**, 737 (1979)
2. G. Bertin, C. C. Lin, S. A. Lowe, R. P. Thurstans: Astrophys. J. **338**, 78 (1989)
3. J. Binney, S. Tremaine: *Galactic Dynamics* (Princeton University Press, Princeton 1987) Chap. 6
4. D. L. Block, G. Bertin, A. Stockton, P. Grosbøl, A. F. M. Moorwood, R. F. Peletier: Astron. Astrophys. **288**, 365 (1994)
5. S. Hozumi, T. Fujiwara, M. T. Nishida: Publ. Astron. Soc. Jpn. **39**, 447 (1987)
6. E. P. Hubble: Astrophys. J. **64**, 321 (1926)
7. A. J. Kalnajs: Astrophys. Lett. **11**, 41 (1972)
8. A. J. Kalnajs: Astrophys. J. **175**, 63 (1972)
9. C. C. Lin, F. H. Shu: Astrophys. J. **140**, 646 (1964)
10. B. Lindblad: Stockholm Observ. Ann. **22**, 3 (1963)
11. J. Ma: Astron. Astrophys. **388**, 389 (2002)
12. M. Miyamoto: Publ. Astron. Soc. Jpn. **23**, 21 (1971)
13. M. T. Nishida, Y. Watanabe, T. Fujiwara, S. Kato: Publ. Astron. Soc. Jpn. **36**, 27 (1984)
14. H. C. Plummer: Mon. Not. R. Astro. Soc. **71**, 460 (1911)
15. W. W. Roberts: Astrophys. J. **158**, 123 (1969)
16. M. S. Roberts, M. P. Haynes: Annu. Rev. Astron. Astrophys. **32**, 115 (1994)
17. W. W. Roberts, Jr., M. S. Roberts, F. H. Shu: Astrophys. J. **196**, 381 (1975)
18. A. Toomre: Astrophys. J. **138**, 385 (1963)
19. A. Toomre: Astrophys. J. **139**, 1217 (1964)
20. A. Toomre: Astrophys. J. **158**, 899 (1969)
21. A. Toomre: 'What amplifies the spirals'. In: *The Structure and Evolution of Normal Galaxies*, ed. by S.M. Fall, D. Lynden-Bell (Cambridge University Press, Cambridge 1981) pp. 111–136